Supporting Information

Experimental section

The synthesis of Pd metallene

40.0 mg Sodium tetrachloropalladate (II) (Na_2PdCl_4, 98%) was dissolved into 100.0 mL methanol. After stirring for 10 min, high-purity argon was introduced into the mixture to remove the dissolved oxygen, followed by heating to 60°C. Then the mixture was bubbled with carbon monoxide for 15 min. The collected sediment was centrifuged and washed with mixed solution of ethanol and deionized water for several times. The obtained sample was denoted as Pd metallene.

The preparation of E-Pd metallene

The prepared Pd metallene was added into 30 mL of acetic acid (0.5 mol L^{-1}) solution, followed by bubbling with high-purity argon for 15 min. The mixture was then placed in a 50 mL Teflon-sealed autoclave and maintained at 100°C for 6 h. After centrifuging and washing with ethanol for several times, the collected product was named as E-Pd metallene.

The synthesis of carbon supported Pd nanoparticles

30 mg Vulcan XC-72 carbon, 62.8 mg poly(vinyl pyrrolidone), and 36 mg L-ascorbic acid were dispersed into 10 mL of deionized water, followed by heating to 95°C under magnetic stirring. Meanwhile, 28.6 mg ammonium tetrachloropalladate and 45 mg citric acid were dissolved into 1.5 mL of deionized water. Then the aqueous solution was then rapidly injected into the heated mixture. The mixed solution was maintained for 3 h at 95°C, and then cooled down to room temperature. The obtained black power was centrifuged and washed thoroughly with ethanol and deionized water for several times. The collected sample was denoted as carbon supported Pd nanoparticles (PdNPs/C).

The synthesis of carbon supported Pd nanochains

20.0 mg Palladium acetylacetonate, 5.0 mg citric acid, 20.0 mg polyvinylpyrrolidone and 15.0 mg pluronic F-127 were added into 40 mL ethylene glycol under magnetic stirring for around 30 min. The mixture was moved into a stainless-steel autoclave and retained under 120 °C for 2 h, followed by heating to 160 °C for 2 h and further 220 °C for 2 h. After washed three times with deionized water and ethanol for several times, the collected precipitation was named as Pd nanochains. The prepared Pd nanochains and a certain amount of Vulcan XC-72 carbon were dispersed into hexane under ultrasonication for about 30 min. After centrifugated and washed with ethanol for several times, the obtained sample was denoted as carbon supported Pd nanochains (PdNCs/C). The mass ratio for Pd nanochains and Vulcan XC-72 carbon was adjusted to 30:70.

Electrochemical measurements

Electrochemical measurements were conducted on a CHI 760E with a typical three-electrode cell, using a glassy carbon disk electrode (4 mm diameter) as a working electrode, a saturated calomel electrode (SCE) as a reference electrode, and a graphite

rod as counter electrode. To prepare the catalyst ink, 5 mg prepared E-Pd metallene (or Pd metallene) and 20 mg XC-72 carbon were added into the mixture of deionized water (1 mL), isopropanol (3.75 mL), and Nafion (5 wt%, 0.25 mL) solution, followed by ultrasonicating for 30 min. 4 μL catalyst ink was transferred onto a working electrode, and the metal loading is 31.7 μg cm^{-2}. CV curves were tested in 0.5 M H_2SO_4 or 0.5 M H_2SO_4 + 0.5 M HCOOH electrolytes at 50 mV s^{-1}. The Nyquist plots and amperometric i-t curves of Pd-based catalysts were tested as open circuit potentials and 0.05 V (vs. SCE), respectively. The set frequency range is between 100 K Hz and 0.05 Hz.

The ECSA of Pd-based electrocatalysts in this work were calculated using the following equation

$$ECSA = Q / (0.424 \times Pd_m)$$

where Pd_m is the Pd loading on the electrode. The ECSA was calculated by integrating the charges (Q) associated with the peak from reduction of Pd(II) oxide, assuming 0.424 mC cm^{-2} was needed for the reduction of a Pd(II) oxide monolayer.

Calculation method

The density functional theory (DFT) calculations were carried out using the Vienna Ab-initio Simulation Package (VASP)[1-2] with the frozen-core all-electron projector-augment-wave (PAW)[3-4] method. The Perdew-Burke-Ernzerhof (PBE)[5]of generalized gradient approximation (GGA) was adopted to describe the exchange and correlation potential. The cutoff energy for the plane-wave basis set was set to 450 eV. A 5-layer 4×4 Pd(111) plane was built (Pd-plane), and a vacuum region of 15 Å above the plane was used to ensure the decoupling between neighboring systems. The (100) surface of the 4-layer 4×4 Pd(111) slab was used to simulate the edge of Pd(111) slab (Pd-edge), and 3 Pd atoms were removed to build the model of Pd(111) slab with etched edge (Pd-E-edge). The geometry optimizations were performed until the forces on each ion was reduced below 0.01 eV/Å. The 3×3×1 k-point[6] sampling of the Brillouin zone was used. The DFT-D3 method were used to describe the van der Waals interaction[7].

The adsorption energy, E_{ads}, is calculated using the expression

$$E_{ads} = E_{molecule+surface} - E_{surface} - E_{molecule}$$

where $E_{surface}$ is the energy of Pd(111) surface, Pd(111) slab edge, or Pd-vacancy Pd(111) slab edge. $E_{molecule}$ represents the energy of HCOOH. And $E_{molecule+surface}$ represents the total energy of the adsorbed systems.

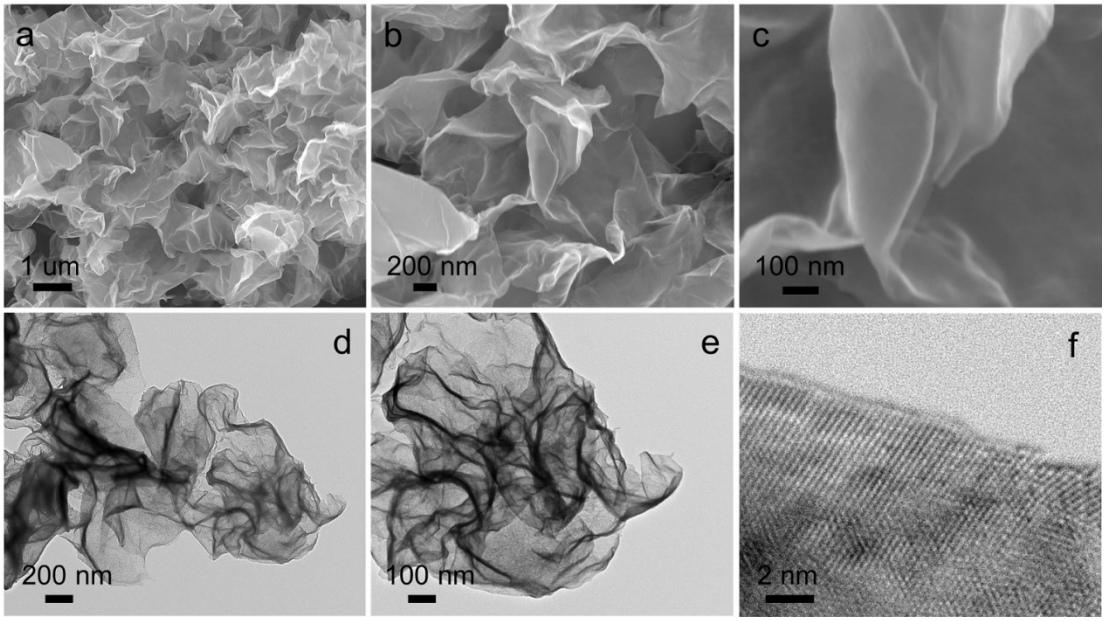

Fig. S1. (a-c) SEM and (d-f) images of Pd metallene.

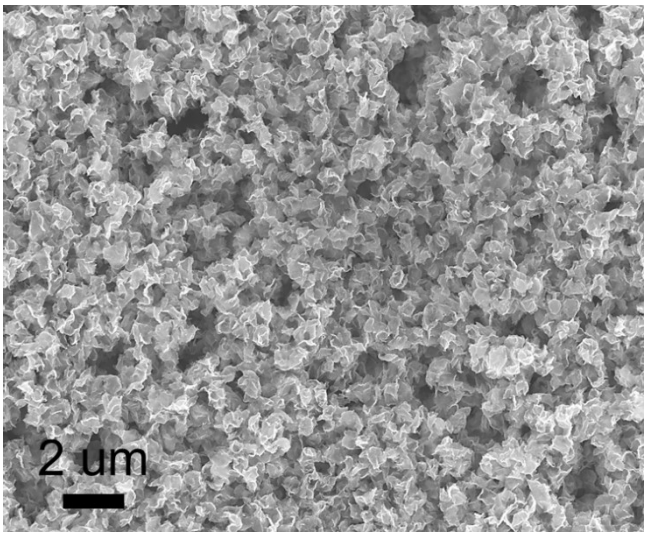

Fig. S2. SEM image of E-Pd metallene.

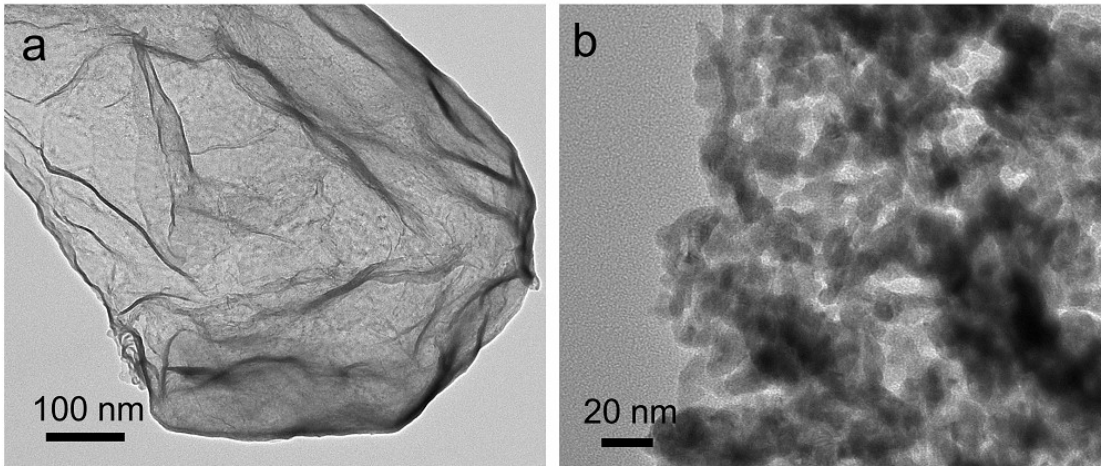

Fig. S3. TEM images of products collected from the reaction with the same conditions used in the synthesis of E-Pd metallene but (a) without adding acetic acid and (b) replacing acetic acid with sulfuric acid (0.5 mol L^{-1}).

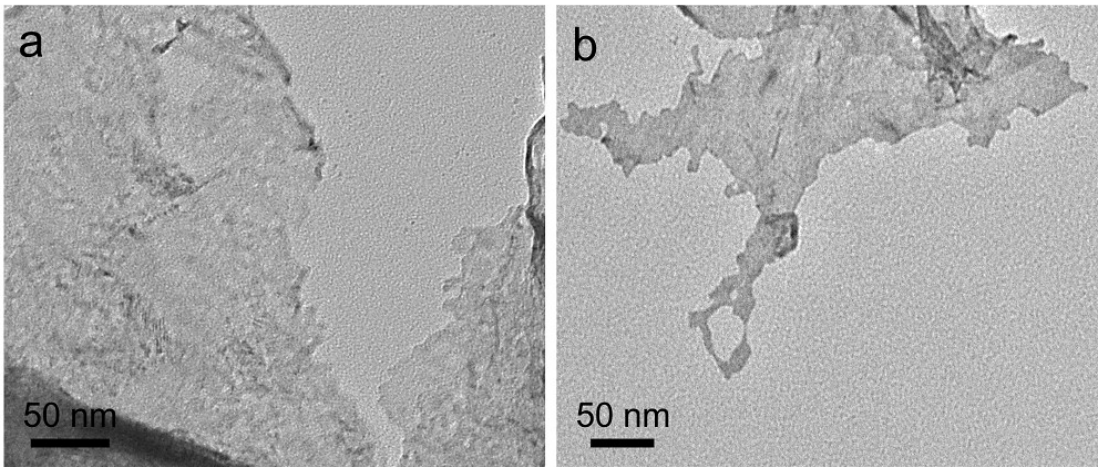

Fig. S4. TEM images of acetic acid treated Pd metallene with (a) 3h and 12h.

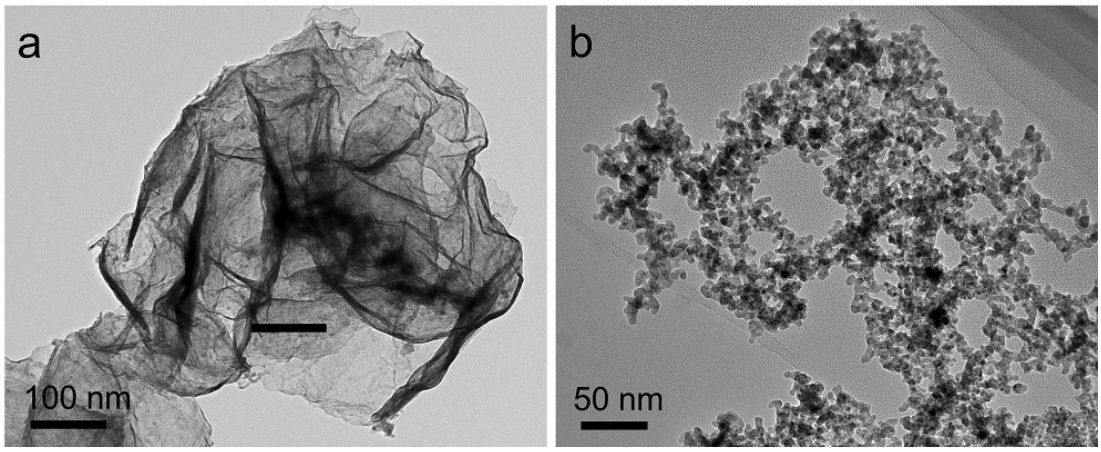

Fig. S5. TEM images of products collected from the reaction with the same conditions used in the synthesis of Pd metallene but replacing methanol with (a) ethanol and (b) deionized water.

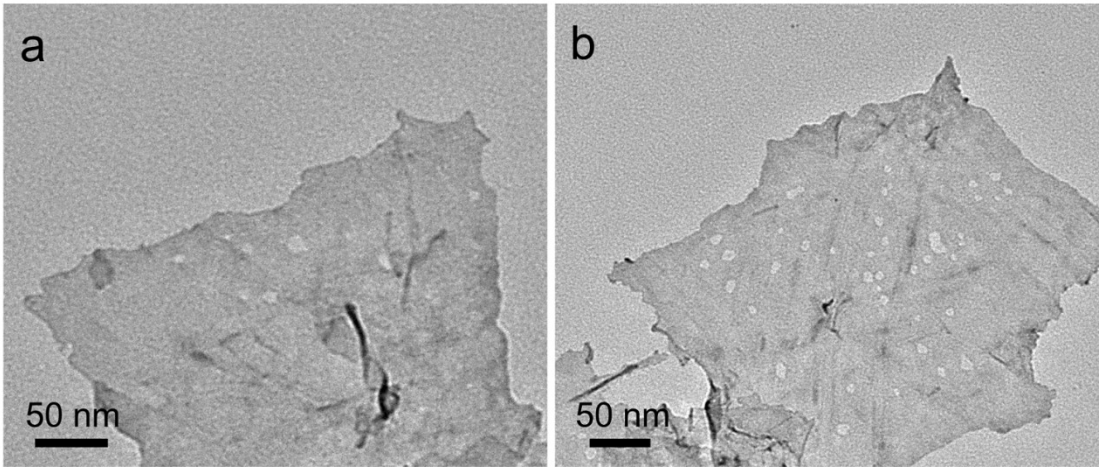

Fig. S6. TEM image of acetic acid treated Pd metallene at (a) 120 ℃ and (b) 150 ℃ for 3h.

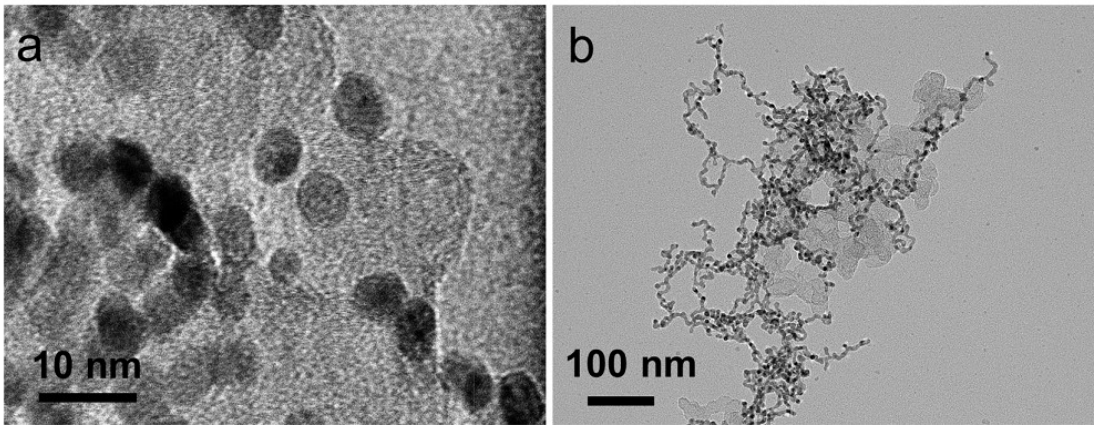

Fig. S7. TEM image of prepared (a) PdNPs/C and (b) Pd NCs/C catalysts.

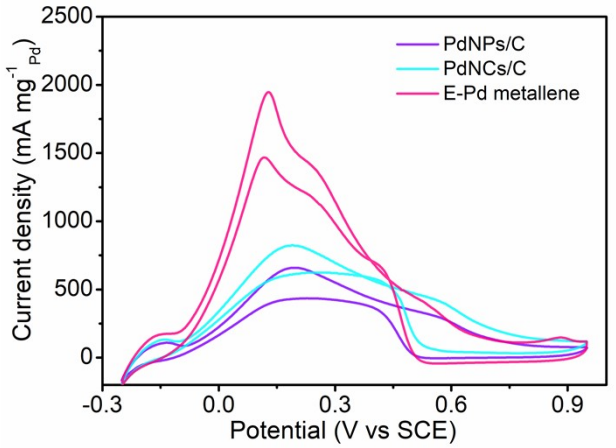

Fig. S8. CV curves of PdNPs/C, Pd NCs/C, and E-Pd metallene in 0.5 M H_2SO_4 + 0.5 M HCOOH electrolyte. Scan rate: 50 mV s^{-1}.

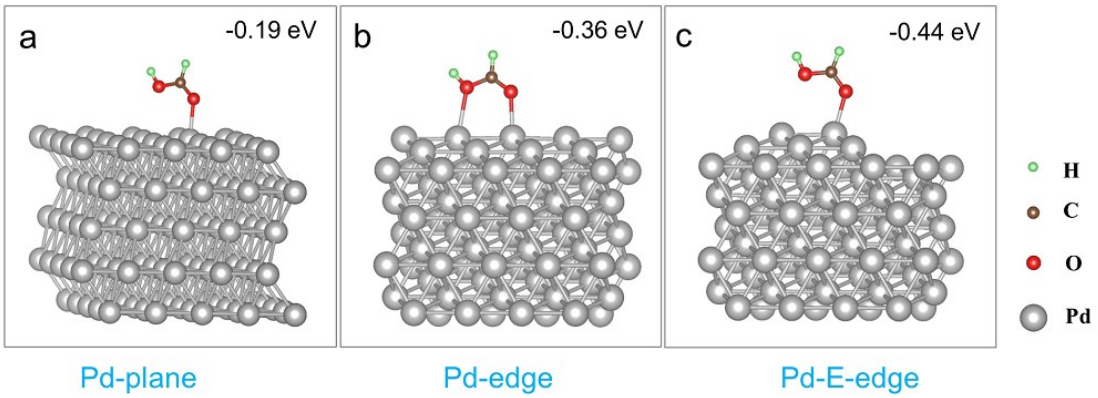

Fig. S9. Optimized adsorption structures of HCOOH on (a) Pd-plane, (b) Pd-edge, and (c) Pd-E-edge, and their corresponding adsorption energies.

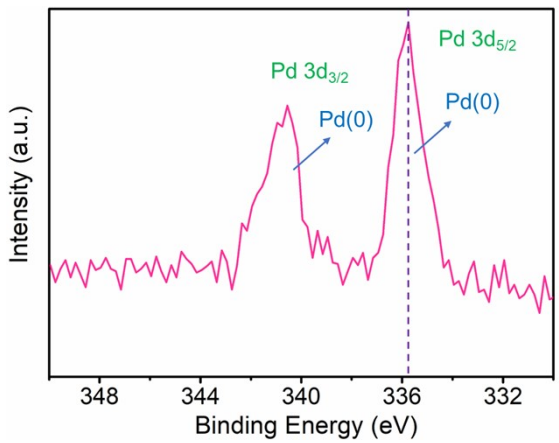

Fig. S10. XPS Pd 3d spectrum of E-Pd metallene after stability testing.

Table S1. The comparison of prepared E-Pd metallene and reported Pd-based catalysts towards formic acid oxidation with respect to ECSA, mass activity, and specific activity.

Catalyst	ECSA $m^2\ g^{-1}_{Pd}$	Mass activity $mA\ mg^{-1}_{Pd}$	Specific activity $A\ m^{-2}$	Reference
E-Pd metallene	117.2	1942.5	16.6	This work
Pd_6Sm_4/rGO	52.7	1089	—	8
WF-PdCu NSs	51	1272.5	6.2	9
Pd_3Fe/C	21.9	696.4	—	10
CuPd@Pd	10.2	501.8	4.9	11
PdRu NSAs	42.8	1100	3.3	12
Coral-like PdCu NPs	36.3	1050	2.9	13
PdCu dendrites	45.7	787.6	1.7	14
PdFe alloy tetrahedrons	17.8	595.8	3.4	15
Pd/NP-Coal-CFs	87.8	536.6	—	16
Pd_3Pt half shells	21.3	318	1.5	17
PdRu NSAs	42.8	1100	—	18
$TNP_{6.67}$@RFC@Pd_1	23.8	905	—	19
Pd_1Cu_1	45.7	786	—	20
PdCu	23.6	1569	—	21
(Pd NSs)	80	1160	—	22
Pd–Mo_2N/rGO	58.1	527	10.4	23
Pd@N-carbon	46	362	—	24
Pd/NG-LCNT	77.6	630	—	25
Pd aerogel	23.4	1791	—	26

References

[1] G. Kresse, J. Hafner. Ab-initio Molecular-Dynamics Simulation of the Liquid-Metal-Amorphous-Semiconductor Transition in Germanium. *Phys. Rev. B* **1994**, *49*, 14251-14269.

[2] G. Kresse, J. Furthmüller. Efficient Iterative Schemes for Ab-initio Total-Energy Calculations using a Plane-Wave Basis Set. *Phys. Rev. B* **1996**, *54*, 11169-11186.

[3] P. E. Blöchl, Projector Augmented-Wave Method. *Phys. Rev. B* **1994**, *50*, 17953-17979.

[4] G. Kresse, D. Joubert. From Ultrasoft Pseudopotentials to the Projector Augmented-Wave Method. *Phys. Rev. B* **1999**, *59*, 1758-1775.

[5] B. Hammer, L. B. Hansen, J. K. Nørskov. Improved Adsorption Energetics within Density-Functional Theory Using Revised Perdew-Burke-Ernzerhof Functionals. *Phys. Rev. B* **1999**, *59*, 7413-7421.

[6] H. J. Monkhorst, J. D. Pack. Special Points for Brillouin-Zone Integrations. *Phys. Rev. B* **1976**, *13*, 5188-5192.

[7] S. Grimme, J. Antony, S. Ehrlich, H. Krieg. A consistent and accurate ab initio parametrization of density functional dispersion correction (DFT-D) for the 94 elements H-Pu. *J. Chem. Phys.* **2010**, *132*, 154104.

[8] M. Yang, M. Pang, J. Chen, F. Gao, H. Li, P. Guo. Surfactant-assisted synthesis of palladium

nanosheets and nanochains for the electrooxidation of ethanol. *ACS Appl. Mater. Interfaces* **2021,** *13*, 9830-9837.

[9] T. Zeng, X. Meng, H. Huang, L. Zheng, H. Chen, Y Zhang, W. Yuan, L.Y. Zhang. Controllable synthesis of web-footed PdCu nanosheets and their electrocatalytic applications. *Small* **2022**, 18, 2107623.

[10] Z. Liu, G. Fu, J. Li, Z. Liu, L. Xu, D. Sun, Y Tang. Facile synthesis based on novel carbon-supported cyanogel of structurally ordered Pd 3 Fe/C as electrocatalyst for formic acid oxidation. *Nano Res.* **2018**, 11, 4686-4696.

[11] Y. Chen, Y. Yang, G. Fu, L. Xu, D Sun., J. M. Lee, Y. Tang. Core–shell CuPd@ Pd tetrahedra with concave structures and Pd-enriched surface boost formic acid oxidation. *J. Mater. Chem. A* **2018**, 10632-10638.

[12] H. Wang, Y. Li, C. Li, Z. Wang, Y. Xu, X. Li, H. Xue, L. Wang. Hyperbranched PdRu nanospine assemblies: an efficient electrocatalyst for formic acid oxidation. *J. Mater. Chem. A* **2018**, 6, 17514-17518.

[13] J. Zheng, H. Zeng, C. Tan, T. Zhang, B. Zhao, W. Guo, H. Wang. Y. Sun, L. Jiang. Coral-like PdCu alloy nanoparticles act as stable electrocatalysts for highly efficient formic acid oxidation. *ACS Sustain. Chem. Eng*. **2019**,18, 15354-15360.

[14] B.Yang, W. Zhang, S. Hu, C. Liu, X. Wang, Y. Fan, Z. Jiang, J. Yang, W. Chen. Bidirectional controlling synthesis of branched PdCu nanoalloys for efficient and robust formic acid oxidation electrocatalysis. *J. Colloid Interf. Sci.* **2021**, 600, 503-512.

[15] B. Cai, Y. Ma, S. Wang, N. Yi, Y. Zheng, X. Qiu, Y. Tang., J. Bao. Facile synthesis of PdFe alloy tetrahedrons for boosting electrocatalytic properties towards formic acid oxidation. *Nanoscale* **2019**, 11, 18015-18020.

[16] M. Lou, R. Wang, J. Zhang, X. Tang, L. Wang, Y. Guo, D. Jia, H. Shi, L. Yang, X. Wang, Z. Sun, T. Wang,Y. Huang. Optimized synthesis of nitrogen and phosphorus dual-doped coal-based carbon fiber supported Pd catalyst with enhanced activities for formic acid electrooxidation. *ACS Appl. Mater. Interfaces* **2019**, 11, 6431-6441.

[17] X. Yan, X. Hu, G. Fu, L. Xu, J. M. Lee, Y. Tang. Facile synthesis of porous Pd3Pt half-shells with rich “active sites” as efficient catalysts for formic acid oxidation. *Small* **2018**, 14, 1703940.

[18] Z. Wang, H. Wang, Z. Zhang, G. Yang, T. He, Y. Yin, M. Jin Synthesis of Pd nanoframes by excavating solid nanocrystals for enhanced catalytic properties. *ACS nano* **2017**, 11, 163-170.

[19] H. Wang, Y. Li, C. Li, Z. Wang, Y. Xu, X. Li, H. Xue, Ll. Wang. Hyperbranched PdRu nanospine assemblies: an efficient electrocatalyst for formic acid oxidation. *J. Mater. Chem. A* **2018**, 6, 17514-17518.

[20] B. Yang, W. Zhang, S. Hu, C. Liu, X. Wang, Y. Fan, Z. Jiang, J. Yang, W. Chen Bidirectional controlling synthesis of branched PdCu nanoalloys for efficient and robust formic acid oxidation electrocatalysis. *J. Colloid Interf. Sci.* **2021**, 600, 503-512.

[21] X. Tai, B. Wu , J. Bao , W. Qu, L. Zhao, Z. Wang Galvanic replacement-mediated synthesis of Pd–Cu alloy nanospheres as electrocatalysts for formic acid oxidation. *Mater. Today* Sustainability **2022**, 18, 100140.

[22] S Zhang, R Xia, Y Su, Y Zou, C Hu, G Yin, E. J. M. Hensen, X Ma, Y Lin. 2D surface induced self-assembly of Pd nanocrystals into nanostrings for enhanced formic acid electrooxidation. *J. Mater. Chem. A* **2020**, 8, 17128-17135.

[23] H. Yan, Y. Jiao, A. Wu, C. Tian, L. Wang, X. Zhang, H. Fu. Synergism of molybdenum nitride and

palladium for high-efficiency formic acid electrooxidation. *J. Mater. Chem. A* **2018**, 6, 7623-7630.
[24] H. Zhang, K. Lu, B. Li, Y. Liu, Y. Su. R. Wang, Y. Cheng. Microfluidic, One-Batch Synthesis of Pd Nanocrystals on N-Doped Carbon in Surfactant-Free Deep Eutectic Solvents for Formic Acid Electrochemical Oxidation. *ACS Appl. Mater. Interfaces* **2020**, 12, 42704-42710.
[25] J. Ren, J. Zhang, C. Yang, Y. Yang, Y. Zhang, F. Yang, R. Ma, L. Yang, H. He, H. Huang. Pd nanocrystals anchored on 3D hybrid architectures constructed from nitrogen-doped graphene and low-defect carbon nanotube as high-performance multifunctional electrocatalysts for formic acid and methanol oxidation. *Mater. Today*. Energy **2020**, 16, 100409.
[26] A.S. Douk, H Saravani, M Farsadrooh. Three-dimensional inorganic polymer of Pd aerogel as a highly active support-less anode catalyst toward formic acid oxidation. *Int. J. Hydrog. Energy* **2019**, 44, 18028-18037.